

Symmetry Protected Quantization and Bulk–Edge Correspondence of Massless Dirac Fermions: Application to Fermionic Shastry-Sutherland Model

Toshikaze Kariyado* and Yasuhiro Hatsugai
 Division of Physics, Faculty of Pure and Applied Sciences,
 University of Tsukuba, Tsukuba, Ibaraki 305-8571, Japan
 (Dated: June 5, 2018)

The fermionic Shastry-Sutherland model has a rich phase diagram, including phases with massless Dirac fermions, a quadratic band crossing point, and a pseudospin-1 Weyl fermion. Berry phases defined by the one-dimensional momentum as a parameter are quantized into 0 or π due to the inversion symmetry combined with the time reversal, or existence of the glide plane, which also protects the massless Dirac cones with continuous parameters. This is the symmetry protected Z_2 quantization. We have further demonstrated the Z_2 Berry phases generically determine the existence of edge states in various phases and with different types of the boundaries as the bulk–edge correspondence of the massless Dirac fermion systems.

PACS numbers: 73.20.-r, 03.65.Vf

Massless Dirac fermion systems, which are zero gap semiconductors found in various situations[1–5] and characterized by a linear dispersion, are novel semimetallic materials exhibiting many intriguing phenomena. A typical realization of massless Dirac fermion system is celebrated graphene[1], which has been attracted much attention since its discovery. Not only in conventional solid state materials, but also in optical lattice systems, the fabrication of massless Dirac fermions becomes a hot topic very recently[6, 7]. Among the many unusual properties of the massless Dirac fermions, appearance of characteristic edge states[8–10] is important in the view of the bulk–edge correspondence, which implies that topologically nontrivial bulk states and appearance of the edge states, i.e., localized modes near the boundaries, are closely related and reflect each others. The concept “bulk–edge correspondence” is established for a topologically nontrivial gapped state[11]. There, a bulk topological number and number of edge states are connected. Actually, although the massless Dirac fermion system is gapless at the Fermi energy and a topological number cannot be well defined, the bulk–edge correspondence is still at work[9, 12, 13].

Instead of the bulk topological number such as the Chern number, the Berry phase $\theta(k_{\parallel})$ plays a central role in the massless Dirac fermion systems[9, 12, 13]. Here, $\theta(k_{\parallel})$ is a bulk quantity parameterized by a momentum k_{\parallel} , which is parallel to the “edge”. Generically the Berry phase $\theta(k_{\parallel})$ is gauge dependent and takes any real number in modulo 2π . It is in contrast to the Chern number that is gauge invariant and intrinsically integer[14]. However, with the help of a supplemental symmetry, the Berry phase is quantized and becomes topological, that is, adiabatic invariant[12, 15–18]. This is the symmetry protected quantization, which is useful in odd dimension. Note that the Chern number and its generalizations are only well defined in even dimensions.

The symmetry further plays a crucial role for the topological stability of the massless Dirac fermions. Since the gap closing point has co-dimension 3[17, 19], the symmetry discussed above is crucial to have a massless Dirac fermions in two-dimensions in a generic situation.

As for the bulk–edge correspondence of the massless Dirac fermions and the stability of the doubled Dirac cones, the chiral symmetry is often employed[9, 12]. In this paper, with general discrete symmetries, the idea on the bulk–edge correspondence of the massless Dirac fermions and its stability are discussed and demonstrated using the fermionic Shastry-Sutherland (SS) model. This model has not been studied well, while a *spin* model on the SS lattice, which is known as the orthogonal dimer model, has been extensively studied following the discovery of the exact ground state wave function[20–23], and has been realized experimentally[24]. In the following, we first show that the fermionic SS model has a rich electronic phase diagram. Interestingly, the phases with massless Dirac fermions, a quadratic band crossing point[25], or a pseudospin-1 Weyl fermion[26, 27] at the Fermi energy are accessible by controlling only a few parameters. Then the bulk–edge correspondence in the fermionic SS model is discussed, focusing on the phase with massless Dirac fermions. Although the fermionic SS model does not respect the chiral symmetry, existence of the inversion center or the glide plane play crucial role in quantization of the Berry phase and the stability of the massless Dirac fermions.

A possible physical realization of Shastry-Sutherland lattice is visualized as Fig. 1(a). This lattice possesses many symmetries among which the four-fold rotational symmetry, glide plane symmetry, and inversion symmetry play particularly important roles in the following arguments. A simplified picture of the model is shown in Fig. 1(b). A shaded region represents a unit cell, which contains four lattice sites named site 1-4, implying that our model has four bands. Our Hamiltonian is

$$H = \sum_{ab} \sum_{\mathbf{r}\mathbf{r}'} t_{ab}(\mathbf{r} - \mathbf{r}') c_{\mathbf{r}a}^{\dagger} c_{\mathbf{r}'b} = \sum_{abk} (\hat{H}_k)_{ab} c_{ka}^{\dagger} c_{kb}, \quad (1)$$

with $c_{ka} = \frac{1}{\sqrt{N}} \sum_{\mathbf{r}} e^{i\mathbf{k}\cdot\mathbf{r}} c_{\mathbf{r}a}$. Here, indices a and b run from 1 thorough 4, representing four sublattices, while \mathbf{r} and \mathbf{r}' represents lattice vectors on square lattice. We employ four parameters t_+ , t_- , t_x , and t_y that correspond to transfer integrals between the sites connected by bonds indicated as +, –,

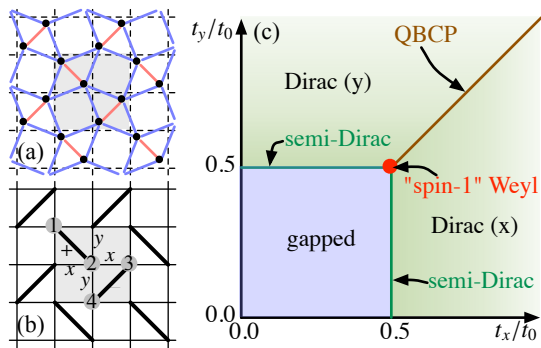


FIG. 1. (a) The most “physical” Shastry-Sutherland lattice. (b) Schematic picture of our model. Bonds named as $+$, $-$, x , and y are associated with the transfer integrals t_+ , t_- , t_x , and t_y , respectively. Shaded region denotes the unit cell. We give numbers one through four to four sites in a unit cell in order to distinguish them. (c) Phase diagram for the case of $t_+ = t_- = t_0$.

x , and y in Fig. 1(b), respectively. The glide plane symmetry is broken when $t_+ \neq t_-$, while the four-fold rotational symmetry is broken when $t_+ \neq t_-$ or $t_x \neq t_y$. In contrast, the inversion symmetry is always kept with this parameterization. For convenience, we also use parameters t_0 , t_1 , Δ_0 , and Δ_1 defined as $t_{\pm} = t_0 \pm \Delta_0$, $t_x = t_1 + \Delta_1$, and $t_y = t_1 - \Delta_1$. In this study, we neglect spin degrees of freedom, and concentrate on the half filled case. Namely, “Fermi energy” appearing in the following refers to the chemical potential achieving half filling, and “gapped state” means that the system has a gap between the second and third lowest bands.

The phase diagram obtained for $\Delta_0 = 0$ ($t_+ = t_-$), which is the case that the two diagonal bonds orthogonal with each other are equivalent, is shown in Fig. 1(c). For $t_x = t_y < 0.5t_0$, the system is in a (trivial) gapped phase. On the other hand, for $t_x = t_y > 0.5t_0$, we find a quadratic band crossing point (QBCP)[25], at which two parabolic bands, one is hole-like and the other is electron-like, touch with each other, at the Γ -point[21, 28]. [Figs. 2(a) and 2(d).] Note that the hole-like band is not parabolic in a strict sense in this case, since it is dispersionless in the Γ - M direction. QBCP is allowed to exist if the system has a four-fold rotational symmetry[29], and has interesting properties. For instance, the four-fold symmetry can be broken by electron-electron interaction effects, leading to emergent nematic phases[25]. For $t_x = t_y = 0.5t_0$, at which the transition between the trivial gapped phase and the phase with QBCP takes place, there exists “pseudospin-1 Weyl fermion”[27], which is characterized by a linear dispersion and a three-fold degeneracy[26], at the Γ -point. [Figs. 2(b) and 2(e).]

A finite Δ_1 ($t_x \neq t_y$) imposed in the QBCP phase immediately leads to a phase with Dirac cones at the Fermi energy. [Figs. 2(c) and 2(f).] Namely, two Dirac cones (and two Dirac points associated with them) are generated as a pair from the QBCP by a finite Δ_1 . The Dirac points are located on the k_x -axis for $\Delta_1 > 0$, while they are on the k_y -axis for

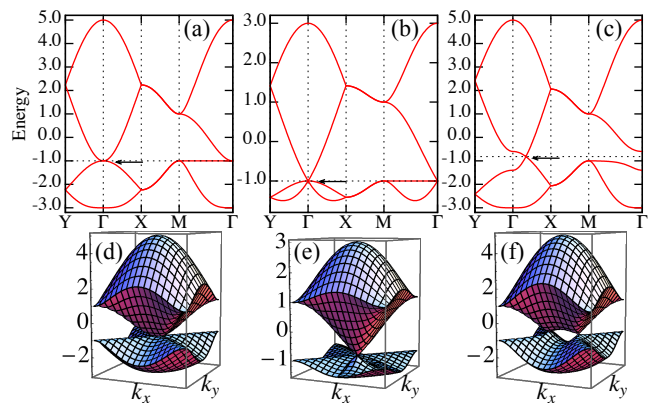


FIG. 2. Band structures and dispersion relations. $(t_0, \Delta_0) = (1.0, 0.0)$ for all three cases, while (t_1, Δ_1) is $(0.0, 0.0)$ (a,d), $(0.5, 0.0)$ (b,e), and $(1.0, 0.1)$ (c,f). In (e), a part of the dispersion is eliminated so that the inside is visible.

$\Delta_1 < 0$. Then, if Δ_1 is continuously modified from positive to negative, the Dirac points first move on the k_x -axis towards the Γ -point until they merge, and they next depart from the Γ -point in the direction of the k_y -axis. Note that the second lowest band is no longer dispersionless on the Γ - M direction [Fig. 2(c)], which is important for letting the Dirac fermions being the only feature appearing at the Fermi energy. If t_1 is made smaller and smaller with finite Δ_1 , the system experiences a transition from the phase with Dirac cone to the trivial gapped phase. The transition between two phases is characterized by an appearance of a semi-Dirac fermion, whose dispersion is linear in one direction and parabolic in the other direction. Actually, this type of disappearance of the Dirac cones is rather general and found in many other models for Dirac fermions[30].

When $\Delta_0 \neq 0$ simultaneously with $\Delta_1 \neq 0$, the Dirac points go into the general points in the Brillouin zone apart from the high-symmetry lines, i.e., the k_x - and k_y -axes. In this case, the symmetry of the system is much lowered, but the inversion (and time reversal) symmetry is still kept. We will see later that this is sufficient for stabilizing the massless Dirac fermions by means of the quantized Berry phase. In Fig. 3, the trajectories of the Dirac points when (Δ_0, Δ_1) is changed according to $(\Delta_0, \Delta_1) = (\delta_0 \sin \phi, \delta_1 \cos \phi)$ ($0 \leq \phi \leq 2\pi$) are illustrated for $t_0 = t_1 = 1.0$ and $(\delta_0, \delta_1) = (0.1, 0.1)$ or $(0.2, 0.1)$. We find that the Dirac points wind around the Γ -point as ϕ grows from 0 to 2π . Note that the physical state gets back to the original state after 2π change in ϕ , but each Dirac point does not get back to the original position: two Dirac points interchange their position after 2π change in ϕ . It is also worth noting that once the fermionic Shastry-Sutherland model is realized in some materials, perturbations leading to $\Delta_0 \neq 0$ and $\Delta_1 \neq 0$ can be induced by applying uniaxial pressure in diagonal or rectangular direction.

Now, let us discuss the bulk–edge correspondence of the massless Dirac fermions. For this purpose, we calculate edge

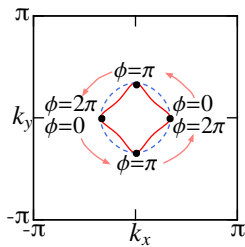


FIG. 3. Trajectories of Dirac points for $(\Delta_0, \Delta_1) = (\delta_0 \sin \phi, \delta_1 \cos \phi)$ with $t_0 = t_1 = 1.0$. Solid line is for $(\delta_0, \delta_1) = (0.1, 0.1)$ while dashed line is for $(\delta_0, \delta_1) = (0.2, 0.1)$.

spectra and Berry phase for fermionic Shastry-Sutherland model. For simplicity, we discuss the edge parallel to the x -axis, but it is possible to extend the following methods to more general cases[13]. Edge spectra are calculated by making the system with strip (or ribbon) geometries. Here, in order to make a direct connection to the Berry phase arguments, we set a rule to make strips for calculation: edges are given by cutting a periodic system *in between the unit cells*. With this construction, the edge shapes, or how the system is terminated at the edge, crucially depend on the convention of the unit cell since the position of the cut is fixed in between the unit cells. In this letter, we treat two kinds of unit cell conventions that lead to two kinds of edge terminations, illustrated as Fig. 4(a) and Fig. 4(b), respectively. Hereafter, we call the convention in Figs. 4(a) and 4(b) “type 1” and “type 2”, respectively. As we limit our attention to the edge parallel to the x -axis, Berry phase[12, 13, 15] is defined as

$$i\theta(k_{\parallel}) = \sum_{n \in \text{filled}} \int_{-\pi}^{\pi} dk_{\perp} \langle u_{nk_{\parallel}k_{\perp}} | \nabla_{k_{\perp}} | u_{nk_{\parallel}k_{\perp}} \rangle, \quad (2)$$

where k_{\parallel} and k_{\perp} are essentially k_x and k_y , and $|u_{nk_{\parallel}k_{\perp}}\rangle$ is a Bloch wave function that is a four-component vector for our four-band tight-binding model. Although we handle a two-dimensional model here, the extension to d dimensional cases is straight forward. Namely, we simply regard k_{\parallel} as a $d - 1$ dimensional vector rather than a number. Actual evaluation of Eq. (2) is performed using a technique in Refs. 31 and 32.

Calculated edge spectra and $\theta(k_{\parallel})/2\pi$ for type 1 and type 2 conventions with $(t_0, t_1, \Delta_0, \Delta_1) = (1.0, 1.0, 0.0, 0.1)$ are plotted as functions of k_{\parallel} in Figs. 4(c) and 4(d). From these figures, we can extract three important points: (1) appearance of edge states, (2) quantization of the Berry phase, and (3) an intimate relation between the edge states and the Berry phase. We explain these in turn in the following.

Since we chose the parameters so as to have bulk massless Dirac fermions, bulk continuum, which is the filled region in Figs. 4(c) and 4(d) and contributed from the bulk states, becomes gapless at the projected Dirac points. We find the edge states apart from the bulk continuum connecting the projected Dirac points for both of the type 1 and 2 cases. The edge states for the type 1 and 2 cases are different due to the different edge termination. For the type 1 case, the edge state appears near

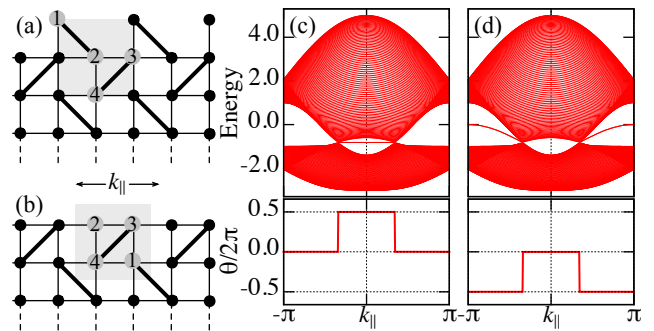


FIG. 4. (a,b) Unit cell conventions and edge shapes. (c,d) Edge spectra and Berry phase $\theta(k_{\parallel})$ divided by 2π as functions of k_{\parallel} for $(t_0, t_1, \Delta_0, \Delta_1) = (1.0, 1.0, 0.0, 0.1)$. (c) is for type 1 edge (a), while (d) is for type 2 edge (b).

$k_{\parallel}(=k_x)=0$, while for the type 2 case, it appears near $k_{\parallel} = \pi$. For both cases, the edge states are dispersive since there is no chiral symmetry that limits the energy of the edge states, but the edge state shows almost flat dispersion for the type 1 case.

In general, the quantization of the Berry phase is caused by some symmetry. In the case of Eq. (2), it is proven that the combination of the time reversal and inversion symmetries is important. These symmetries force $\theta(k_{\parallel})$ to obey

$$\theta(k_{\parallel}) = -\theta(k_{\parallel}) + 2\pi l - 2\pi \Delta^l(k_{\parallel}), \quad (3)$$

where

$$\Delta^l(k_{\parallel}) = \sum_{n \in \text{filled}} \frac{1}{2\pi} \int_{-\pi}^{\pi} dk_{\perp} i \langle u_{nk_{\parallel}k_{\perp}} | \hat{P}_{\mathbf{k}}^{-1} (\partial_{k_{\perp}} \hat{P}_{\mathbf{k}}) | u_{nk_{\parallel}k_{\perp}} \rangle \quad (4)$$

with l being an integer and $\hat{P}_{\mathbf{k}}$ being the inversion symmetry operator satisfying $\hat{H}_{-\mathbf{k}} = \hat{P}_{\mathbf{k}} \hat{H}_{\mathbf{k}} \hat{P}_{\mathbf{k}}^{-1}$. Then, if $\Delta^l(k_{\parallel})$ is zero (because $\hat{P}_{\mathbf{k}}$ has no \mathbf{k} dependence, for instance) or some integer (by some symmetrical reason), $\theta(k_{\parallel})$ becomes quantized to 0 or π , i.e., Z_2 . Note that the inversion symmetry alone is sufficient for one-dimensional models[15], but it must be combined with the time reversal symmetry for higher dimensional cases. Note also that the reflection symmetry whose reflection plane is parallel to the edge alone can quantize $\theta(k_{\parallel})$. In the case of fermionic SS model, the glide plane symmetry existing if $t_+ = t_-$, plays a role of the reflection plane symmetry.

A physical meaning of the Z_2 quantization can be understood from the fact that $\theta(k_{\parallel})$ has close relation to the electronic polarization[31]. The inversion or reflection symmetry gives restrictions for possible values of the electronic polarization, and these restrictions appear as the Z_2 quantization. However, a special attention is required in the case that the bulk symmetries are broken after introducing edges to the system. In our edge construction, edge shapes depend on the unit cell convention. Then, if we calculate $\theta(k_{\parallel})$ using a unit cell convention that leads to an edge breaking bulk inversion and glide plane symmetries, $\theta(k_{\parallel})$ is not necessarily quantized even

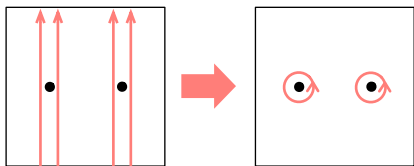


FIG. 5. Schematic description of the relation between π -jumps in $\theta(k_{\parallel})$ and Dirac points.

if bulk system without edges has inversion and glide plane symmetries. This corresponds to the case that $\Delta^I(k_{\parallel})$ is noninteger.

The stability of massless Dirac fermions in two-dimensional systems can be clearly addressed using the quantized $\theta(k_{\parallel})$, which we call Z_2 Berry phase. In order to see this, we must realize that π -jump in $\theta(k_{\parallel})$ is directly related to a bulk Dirac fermion. If an infinitesimal change in k_{\parallel} , $k_{\parallel} \rightarrow k_{\parallel} + \delta k$ gives a finite change between $\theta(k_{\parallel})$ and $\theta(k_{\parallel} + \delta k)$, the electronic dispersion should have a singularity in the area enclosed by the two integration paths for $\theta(k_{\parallel})$ and $\theta(k_{\parallel} + \delta k)$, but, a massless Dirac fermion is nothing more than a singularity in the electronic dispersion. Furthermore, the value π is exactly Berry phase acquired when the integration path encloses a Dirac point. The idea is described in Fig. 5 as a deformation of the integration path. Then, as far as the symmetries quantizing $\theta(k_{\parallel})$ are preserved, massless Dirac fermions are topologically stable, since π -jump cannot be suddenly removed by a small change in parameters when $\theta(k_{\parallel})$ is quantized to 0 or π : π -jump only disappears when two jumps are merged, or parameters themselves are discontinuously changed. Inversely speaking, if symmetries preserving $\theta(k_{\parallel})$ -quantization is broken, massless Dirac fermion will be no longer stable. In fact, we have checked that when extra terms breaking the inversion and glide plane symmetries are added to the fermionic SS model, $\theta(k_{\parallel})$ deviates from 0 or π , and a gap is induced at the Dirac point.

Z_2 Berry phase is also useful in making a criterion for the existence of massless Dirac fermions in a given model[33, 34]. As discussed in Refs. 35 and 36, there is no need to explore the entire Brillouin zone to find out Dirac points, thanks to the Z_2 quantization. Instead, it is sufficient to check the values of $\theta(k_{\parallel})$ at two k_{\parallel} s, typically at $k_{\parallel} = 0$ and π . If two $\theta(k_{\parallel})$ take different values, there must be at least one jump, or equivalently, Dirac point, as far as the quantization is retained.

The close relation between the appearance of edge states and $\theta(k_{\parallel})$ can be seen in Figs. 4(c) and 4(d). Namely, we find edge states for k_{\parallel} with $\theta(k_{\parallel}) = \pi \bmod 2\pi$, while no edge states for k_{\parallel} with $\theta(k_{\parallel}) = 0$. Since the π -jumps are related to the bulk Dirac points, existence and nonexistence of the edge states is switched at the Dirac points projected to the edge. Here, we want to emphasize that, although $\theta(k_{\parallel})$ can be calculated only with bulk information, $\theta(k_{\parallel})$ apparently has an ability to capture the difference in edge terminations, i.e., difference between type 1 and type 2 edges. This is because $\theta(k_{\parallel})$ does

depend on the choice of the basis set since its definition involves the Bloch wave functions, and different unit cell conventions are actually connected by a unitary transformation, i.e., a transformation of the basis set. In our specific case, $\theta(k_{\parallel})$ in type 1 and type 2 conventions are connected as

$$\theta_{\text{type 2}}(k_{\parallel}) = \theta_{\text{type 1}}(k_{\parallel}) - 2\pi\rho_1(k_{\parallel}), \quad (5)$$

where $\rho_1(k_{\parallel})$ is k_{\parallel} resolved filling of site 1, which is explicitly calculated as

$$\rho_1(k_x) = \sum_{n \in \text{filled}} \frac{1}{2\pi} \int_{-\pi}^{\pi} dk_y \langle u_{nk_x, k_y} | P_1 | u_{nk_x, k_y} \rangle. \quad (6)$$

Here, P_1 is a projection operator projecting on the site 1 component. As far as $t_+ = t_-$, $\rho_1(k_{\parallel}) = 0.5$ holds in our model by a symmetrical reason. Consequently, $\theta_{\text{type 1}}(k_{\parallel})$ and $\theta_{\text{type 2}}(k_{\parallel})$ differ by π .

Intuitive understanding of this bulk–edge correspondence is possible with the help of adiabatic continuation when $\theta(k_{\parallel})$ is quantized. We briefly explain this for the type 2 edge with parameters used in Fig. 4(d). Recall that the type 2 edge shows the edge states for $k_{\parallel} = \pi$ and no edge state for $k_{\parallel} = 0$. If k_{\parallel} is fixed to π , k resolved Hamiltonian \hat{H}_k can be adiabatically deformed *without gap closing and keeping $\theta(k_{\parallel})$ value* to the Hamiltonian corresponding to $t_x = t_y = 0$. Then, edge states are readily understood as dangling states appearing as a result of cutting remained diagonal bonds for type 2 edge. Importantly, the same adiabatic continuation cannot be applied to $k_{\parallel} = 0$ case since it leads to the gap closing, which allows change in quantized $\theta(k_{\parallel})$ and leads to qualitative changes of the system properties. We have to use different adiabatic continuation, and that continuation should give Hamiltonian without dangling states for the type 2 edge.

In summary, we have shown that the fermionic SS model is a quite important model which hosts many peculiar phases including the phase with Dirac cones. Since the spin SS model has been materialized, we believe that it is possible to realize a fermionic counterpart. Alternatively, the model may be realized in some optical lattices. Using the SS model, we have also demonstrated roles of the symmetry for the massless Dirac fermions and the Z_2 quantization of the Berry phase, which also provides the bulk–edge correspondence.

This work is partly supported by Grants-in-Aid for Scientific Research, No.23340112, No.25610101, and No.23540460 from JSPS.

* kariyado.t.gf@u.tsukuba.ac.jp

- [1] K. S. Novoselov, A. K. Geim, S. V. Morozov, D. Jiang, M. I. Katsnelson, I. V. Grigorieva, S. V. Dubonos, and A. A. Firsov, *Nature* **438**, 197 (2005).
- [2] S. Katayama, A. Kobayashi, and Y. Suzumura, *J. Phys. Soc. Jpn.* **75**, 054705 (2006).
- [3] M. Z. Hasan and C. L. Kane, *Rev. Mod. Phys.* **82**, 3045 (2010).
- [4] X.-L. Qi and S.-C. Zhang, *Rev. Mod. Phys.* **83**, 1057 (2011).

- [5] J. Moore, *Nat Phys* **5**, 378 (2009).
- [6] N. Goldman, A. Kubasiak, A. Bermudez, P. Gaspard, M. Lewenstein, and M. A. Martin-Delgado, *Phys. Rev. Lett.* **103**, 035301 (2009).
- [7] L. Tarruell, D. Greif, T. Uehlinger, G. Jotzu, and T. Esslinger, *Nature* **483**, 302 (2012).
- [8] M. Fujita, K. Wakabayashi, K. Nakada, and K. Kusakabe, *J. Phys. Soc. Jpn.* **65**, 1920 (1996).
- [9] S. Ryu and Y. Hatsugai, *Phys. Rev. Lett.* **89**, 077002 (2002).
- [10] T. Kariyado and M. Ogata, *J. Phys. Soc. Jpn.* **81**, 064701 (2012).
- [11] Y. Hatsugai, *Phys. Rev. Lett.* **71**, 3697 (1993).
- [12] Y. Hatsugai, *Solid State Commun.* **149**, 1061 (2009).
- [13] P. Delplace, D. Ullmo, and G. Montambaux, *Phys. Rev. B* **84**, 195452 (2011).
- [14] D. J. Thouless, M. Kohmoto, M. P. Nightingale, and M. den Nijs, *Phys. Rev. Lett.* **49**, 405 (1982).
- [15] J. Zak, *Phys. Rev. Lett.* **62**, 2747 (1989).
- [16] Y. Hatsugai, *J. Phys. Soc. Jpn.* **75**, 123601 (2006).
- [17] Y. Hatsugai, *New J. Phys.* **12**, 065004 (2010).
- [18] T. Fukui, K.-I. Imura, and Y. Hatsugai, *J. Phys. Soc. Jpn.* **82**, 073708 (2013).
- [19] M. V. Berry, *Proc. R. Soc. A* **392**, 45 (1984).
- [20] B. S. Shastry and B. Sutherland, *Physica B+C* **108**, 1069 (1981).
- [21] B. S. Shastry and B. Kumer, *Prog. Theor. Phys. Supplement* **145**, 1 (2002).
- [22] S. Miyahara and K. Ueda, *J. Phys.: Condens. Matter* **15**, R327 (2003).
- [23] I. Maruyama, S. Tanaya, M. Arikawa, and Y. Hatsugai, *J. Phys.: Conference Series* **320**, 012019 (2011).
- [24] H. Kageyama, K. Yoshimura, R. Stern, N. V. Mushnikov, K. Onizuka, M. Kato, K. Kosuge, C. P. Slichter, T. Goto, and Y. Ueda, *Phys. Rev. Lett.* **82**, 3168 (1999).
- [25] K. Sun, H. Yao, E. Fradkin, and S. A. Kivelson, *Phys. Rev. Lett.* **103**, 046811 (2009).
- [26] E. Dagotto, E. Fradkin, and A. Moreo, *Phys. Lett. B* **172**, 383 (1986).
- [27] Z. Lan, N. Goldman, and P. Öhberg, *Phys. Rev. B* **85**, 155451 (2012).
- [28] J. Liu, N. Trivedi, Y. Lee, B. N. Harmon, and J. Schmalian, *Phys. Rev. Lett.* **99**, 227003 (2007).
- [29] K. Sun, W. V. Liu, A. Hemmerich, and S. Das Sarma, *Nat Phys* **8**, 67 (2012).
- [30] G. Montambaux, F. Piéchon, J.-N. Fuchs, and M. O. Goerbig, *Eur. Phys. J. B* **72**, 509 (2009).
- [31] R. D. King-Smith and D. Vanderbilt, *Phys. Rev. B* **47**, 1651 (1993).
- [32] T. Hirano, H. Katsura, and Y. Hatsugai, *Phys. Rev. B* **78**, 054431 (2008).
- [33] C. Herring, *Phys. Rev.* **52**, 365 (1937).
- [34] K. Asano and C. Hotta, *Phys. Rev. B* **83**, 245125 (2011).
- [35] T. Mori, *J. Phys. Soc. Jpn.* **82**, 034712 (2013).
- [36] F. Piéchon and Y. Suzumura, *J. Phys. Soc. Jpn.* **82**, 033703 (2013).